

# Journal of Materials Chemistry B

Accepted Manuscript



This is an *Accepted Manuscript*, which has been through the Royal Society of Chemistry peer review process and has been accepted for publication.

*Accepted Manuscripts* are published online shortly after acceptance, before technical editing, formatting and proof reading. Using this free service, authors can make their results available to the community, in citable form, before we publish the edited article. We will replace this *Accepted Manuscript* with the edited and formatted *Advance Article* as soon as it is available.

You can find more information about *Accepted Manuscripts* in the [Information for Authors](#).

Please note that technical editing may introduce minor changes to the text and/or graphics, which may alter content. The journal's standard [Terms & Conditions](#) and the [Ethical guidelines](#) still apply. In no event shall the Royal Society of Chemistry be held responsible for any errors or omissions in this *Accepted Manuscript* or any consequences arising from the use of any information it contains.



Journal Name

ARTICLE

## A Dual-Emission Fluorescence-Enhanced Probe for Imaging Copper(II) Ions in Lysosomes

Mingguang Ren, Beibei Deng, Jian-Yong Wang, Zhan-Rong Liu, Weiyin Lin\*

Received 00th January 20xx,  
Accepted 00th January 20xx

DOI: 10.1039/x0xx00000x

www.rsc.org/

We have developed the first example of a fluorescence-enhanced and lysosome-targeted  $\text{Cu}^{2+}$  probe (**Lys-Cu**) with unique dual-channel emissions. The new synthesized fluorescent probe **Lys-Cu** which contains two recognition sites with different sensing mechanism to  $\text{Cu}^{2+}$ , displays fluorescence-enhanced dual-channel emissions with fluorescence response to  $\text{Cu}^{2+}$  under lysosome pH environment. Fluorescence imaging shows that **Lys-Cu** is membrane-permeable and suitable for visualization of  $\text{Cu}^{2+}$  in lysosomes of living cells with dual-channel imaging.

### Introduction

Copper is the third-most abundant transition metal in human body and plays an important role in various physiologic processes. Copper in the cytoplasm for the most part binds to metallothionein, but the excess copper is excreted into the bile mainly through a lysosome-to-bile pathway.<sup>1</sup> Disruption of copper homeostasis is closely related to a number of neurodegenerative diseases, including Wilson's disease (WD),<sup>2</sup> Menkes disease (MD)<sup>3</sup> and Alzheimer's disease (AD).<sup>4</sup> Moreover, long-term exposure to high levels of  $\text{Cu}^{2+}$  can induce liver and kidney damage. Copper commonly accumulates in the lysosomes of patients in WD's later stage, and the amyloid precursor protein (APP), which works as a  $\text{Cu}^{2+}$  transporter of AD, is known to be degraded in lysosomes. Recently, Human copper transporter (hCTR)2 localized in late endosomes and lysosomes facilitates cellular copper uptake.<sup>5</sup> Therefore, it is interesting to study the relationship between copper levels in cells especially in lysosomes and neurological symptoms of disorders of copper metabolism.

Several analytical techniques including atomic absorption spectrometry,<sup>6</sup> inductively coupled plasma atomic emission spectrometry,<sup>7</sup> voltammetry,<sup>8</sup> electrochemical method<sup>9</sup> have been devoted in detection of  $\text{Cu}^{2+}$ . Although these methods are sensitive toward  $\text{Cu}^{2+}$ , they are usually complex and time-consuming and/or need special equipment. Besides, they require complicated sample preparation and extraction of  $\text{Cu}^{2+}$  by means of destruction of tissues or cells, and therefore, these methods are not suitable for living biosystems. In recent years, fluorescent probes, as an excellent detection tools, have attracted increasing attention for high selectivity, high sensitivity, as well as real-time imaging, and they have been widely applied in the detection of anions, cations, and biological molecules.

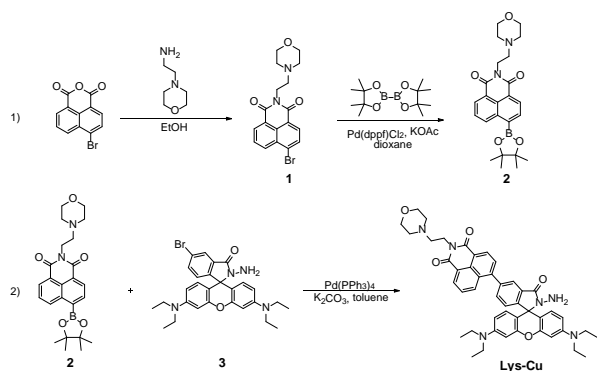
Recently, there have been many outstanding outcomes of detecting  $\text{Cu}^{2+}$  in recent years<sup>10</sup>. However, most of them exhibit changes only in fluorescence intensity<sup>10c-r</sup>, or most of the ratiometric probes exhibit fluorescence signal amplification at one emission wavelength concomitantly with signal reduction at another emission wavelength.<sup>10s-t</sup> By contrast, a dual-channel fluorescence-enhanced probe displays fluorescence enhancement at two emission channels simultaneously upon binding with an analyte. Although dual-channel fluorescence-enhanced probes are exceedingly sought because of their particularly favorable features such as high sensitivity, selectivity, and convenient visible emission assays due to improved signal-to-noise ratio, they are rarely developed with success.

In the past decade, lysosome-targetable fluorescent probes have been constructed for reactive oxygen, nitrogen species, quantifying lysosome pH, cations and viscosity in living cells,<sup>11</sup> implying high importance of lysosomes in cells biology. In addition, the fluorescent probes of  $\text{Cu}^{2+}$  could target to a particular organelle scarce<sup>10p-r</sup>. To the best of our knowledge, no fluorescent probes which are capable of detection of  $\text{Cu}^{2+}$  with fluorescence-enhanced dual-channel emissions in lysosome have been previously constructed.

Ideal fluorescent probes with dual-channel enhanced emissions that can successfully detect  $\text{Cu}^{2+}$  in the lysosomes of living cells are rare. As  $\text{Cu}^{2+}$  plays a critical role in living systems, we were interested in creating  $\text{Cu}^{2+}$  fluorescent probes with dual-channel emissions and localization onto intracellular organelles-lysosomes. To realize this goal, the major challenges include: 1) After responding with  $\text{Cu}^{2+}$ , how to achieve two channels emission at the same time using a single probe molecule. 2) How to make the  $\text{Cu}^{2+}$  probes can locate the organelles of the cell. 3) How to make the  $\text{Cu}^{2+}$  probes overcome the impact of the interfering ions or pH values in organelles.

Herein, we report **Lys-Cu** as a fluorescence-enhanced and lysosome-targeted  $\text{Cu}^{2+}$  probe with unique dual-channel emissions. 1,8-naphthalimide and rhodamine B dyes have been extensively

*Institute of Fluorescent Probes for Biological Imaging, School of Chemistry and Chemical Engineering, School of Biological Science and Technology, University of Jinan, Jinan, Shandong 250022, P.R. China. Email: weiyinlin2013@163.com.*  
Electronic Supplementary Information (ESI) available: Characterization data, and additional spectra. See DOI: 10.1039/x0xx00000x



**Scheme 1** Synthesis of naphthalimide-rhodamine based fluorescent probe of **Lys-Cu**.

employed in fluorescent chemoprobes primarily owing to their excellent photochemical and photophysical properties<sup>12</sup> (Scheme 1). In addition, the carbonyl oxygen atom in 1,8-naphthalimide could participate in coordinating with metal ions. Therefore, 1,8-naphthalimide could play a role both as a fluorophore and a binding unit in probes. Furthermore, rhodamine spirolactam B was selected as the dyes for its target-triggered “turn-on” fluorescent signal that can be easily distinguished, even by the naked eye. The binding of  $\text{Cu}^{2+}$  to probe **Lys-Cu** concurrently switches on two distinct fluorescence emission bands by combination of two signaling mechanisms: suppression of a quenching PET channel and an emissive of rhodamine B ring-opened form channel formation.

## Results and discussion

### Synthesis of **Lys-Cu** fluorescence probe

The synthesis of probe **Lys-Cu** was outlined in Scheme 1. Compounds **1** and **3** were prepared according to a literature procedure.<sup>13</sup> Synthesis of compound **2** was described in the experimental section. The desired product **Lys-Cu** was synthesized from intermediates **2** and **3** by cross-coupling reaction. The structure of compounds **2** and **Lys-Cu** were fully characterized by <sup>1</sup>H NMR, <sup>13</sup>C NMR and HRMS.

### Optical responses of fluorescent probe to $\text{Cu}^{2+}$

With the probe **Lys-Cu** in hand, titrations of the probe (10  $\mu\text{M}$ ) with  $\text{Cu}^{2+}$  were conducted in PBS buffer pH 4.7 (containing 50 %  $\text{CH}_3\text{CN}$  as a cosolvent). As shown in Fig. 1, **Lys-Cu** has nearly no absorption in the visible region (Fig. 1a). This may be attributed to the closed spirolactam form of rhodamine B. Upon reaction with  $\text{Cu}^{2+}$ , however, the red (Fig. 1a inset) color indicative of rhodamine B is greatly restored with the increase of  $\text{Cu}^{2+}$  concentration. With excitation at 360 nm, the free probe **Lys-Cu** displays a weak fluorescent emission band around 440 nm (Fig. 1b) owing to a quenching photoinduced electron-transfer (PET) process from the amino group to the 1,8-naphthalimide fluorophore and the rhodamine B in the ring-closed form. By contrast, addition of  $\text{Cu}^{2+}$  renders the fluorescence intensity a drastic increase in the emission of 440 nm and 580 nm was observed. Consistently, the visual emission color of the probe **Lys-Cu** solution turned from no color to bright orange (Fig. 1b inset).

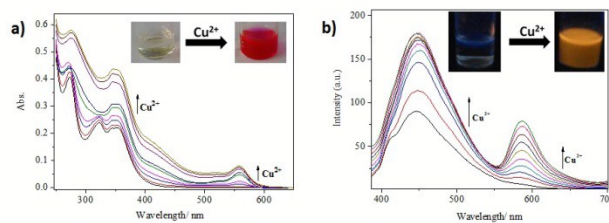
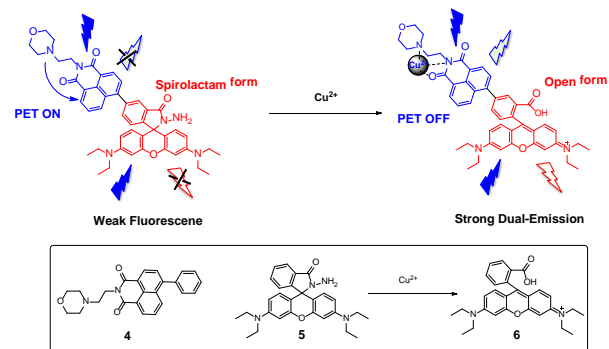


**Fig. 1** The absorption a) and fluorescence b) spectrum changes of probe **Lys-Cu** (10  $\mu\text{M}$ ) upon addition of increasing concentrations of  $\text{Cu}^{2+}$  (0-20 equiv) (Ex = 360 nm) in 20 mM PBS buffer, pH 4.7, containing 50 %  $\text{CH}_3\text{CN}$  as a cosolvent. Inset: the photograph shows the color a) and the fluorescence b) of probe **Lys-Cu** (1 mM) before and after addition of 30 equiv.  $\text{Cu}^{2+}$  in the solution.



**Scheme 2** A proposed novel dual-emission fluorescent probe **Lys-Cu** based on the naphthalimide-rhodamine Platform and structures of control compounds **4**, **5** and **6**.

### Response mechanism of fluorescent probe to $\text{Cu}^{2+}$

The addition of  $\text{Cu}^{2+}$  ions elicits not only a drastic increase in the monomer emission intensity around 440 nm, but also a dramatic fluorescence enhancement around 580 nm. Dual emission mechanism can be expressed by Scheme 2. The new synthesized fluorescent probe **Lys-Cu** contains two recognition sites with different sensing mechanism to  $\text{Cu}^{2+}$  (coordination and reaction mechanism). Coordination of  $\text{Cu}^{2+}$  with the nitrogen atoms may effectively decrease their electron-donating ability, so the quenching PET process from the nitrogen atoms to the 1,8-naphthalimide fluorophore is inhibited, which results in a large increase in fluorescence intensity at 440 nm. This mechanism can be confirmed by the changes of fluorescence (Fig. S1) and <sup>1</sup>H-NMR spectrum (Fig. 2) through titration experiment of the control compound **4**. In addition,  $\text{Cu}^{2+}$  could react and trigger open the spirolactam rhodamine B and the emissive of opened rhodamine B form channel formation, which results in a large increase in fluorescence intensity at 580 nm. Titrations of the control compound **5** (10  $\mu\text{M}$ ) with  $\text{Cu}^{2+}$  and excitation at 360 nm, the fluorescence intensity increased in the emission of 580 nm was also observed (Fig. S2). The comparison of fluorescence spectrum of **Lys-Cu** and the control compounds were shown in Fig. S3. Two emission peaks of the probe **Lys-Cu** have a good overlap with the contrast substance emission peak. By theoretical calculations, in the excited state, 1,8-naphthalimide fluorophore and the rhodamine B were not in the same plane (74° degree angle between the two planes calculated by Gaussian 09) (Fig. 3). Due to a minimal spectrum overlap between the emission spectrum of compound **4** and the absorption spectrum of compound **6** (Fig. 4), the energy cannot be passed from naphthalene amide moiety to rhodamine section. Through-Bond Energy Transfer (TBET) between the chromophores did not exist.

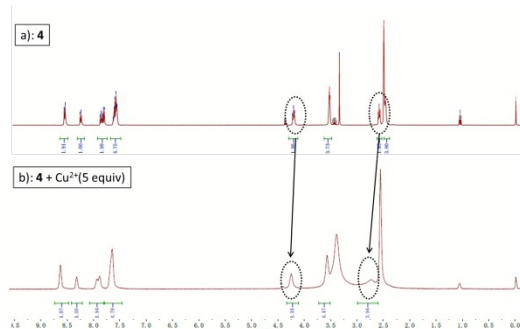


Fig. 2 <sup>1</sup>H NMR spectrum changes with the addition of Cu<sup>2+</sup> (5 equiv) to control compound 4

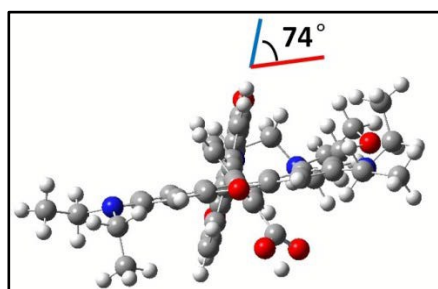


Fig. 3 DFT optimized structure of Lys-Cu. In the ball-and-stick representation, carbon, nitrogen, and oxygen atoms are colored in gray, blue, and red, respectively. H atoms were omitted for clarity. Red line (parallel line of rhodamine plane); blue line (parallel line of naphthalimide plane)

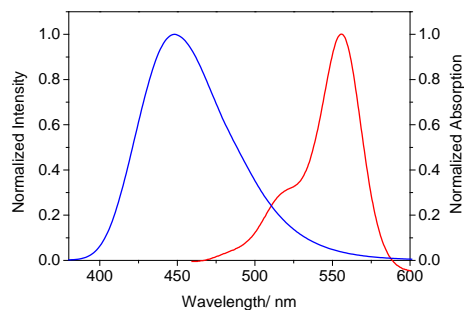


Fig. 4 The comparison of fluorescence spectrum of control compound 4 (blue line) and the absorption spectrum of control compound 6 (red line)

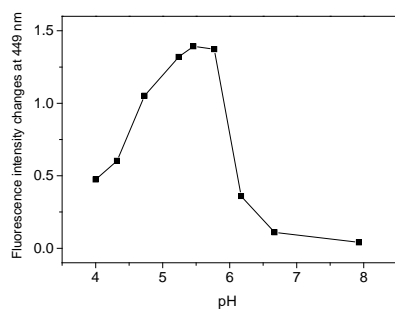


Fig. 5 The emission intensity changes (at 449 nm) of Lys-Cu upon addition of Cu<sup>2+</sup> (20 equiv) at different pH PBS buffer, containing 50 % CH<sub>3</sub>CN as a cosolvent ( $\lambda_{ex}$  = 360 nm).

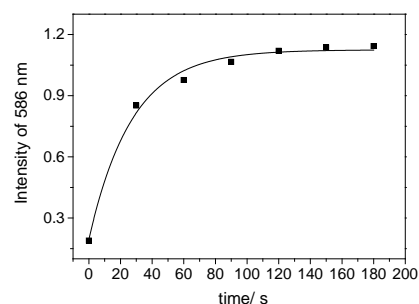


Fig. 6 The fluorescence intensities at 586 nm of Lys-Cu (10 μM) in the presence of Cu<sup>2+</sup> (30 equiv) for continuously monitored at time intervals periods (0-180 s) in PBS buffer, pH 4.7, containing 50% CH<sub>3</sub>CN as a cosolvent. Excitation at 360 nm.

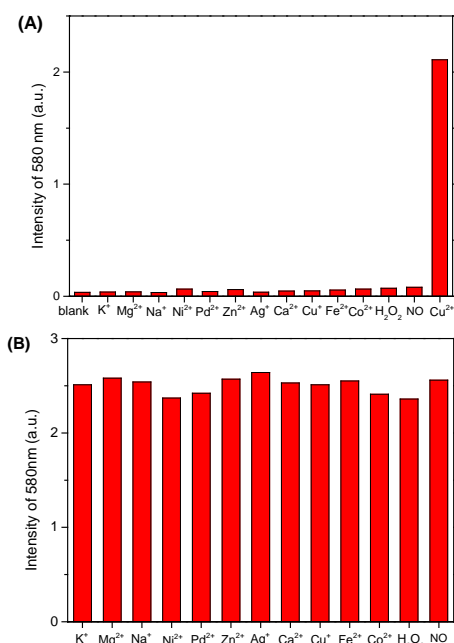


Fig. 7 (A) The fluorescence intensity of probe Lys-Cu (10 mM) at 580 nm in the presence of various analytes (30 equiv) in PBS buffer (pH 4.7, containing 50% CH<sub>3</sub>CN as a cosolvent). (B) The fluorescence intensity of probe Lys-Cu (10 mM) at 580 nm in response to Cu<sup>2+</sup> in the presence of various metal species (30 equiv) in PBS buffer (pH 4.7, containing 50% CH<sub>3</sub>CN as a cosolvent).

### Effect of pH

The pH value of solution has a great influence on the probe response to Cu<sup>2+</sup> (Fig. 5). In the range of 4.0-5.8, we found the fluorescence emission spectrum showed a remarkable enhancement correspondingly in the presence of Cu<sup>2+</sup>. However, in the range of 6.1-9.0, the changes of the fluorescence intensity was not significant in the two emission channels (Fig. S4). As far as we all known, lysosomes contain several types of hydrolytic enzymes, which maintain an acidic luminal pH of ~5.0. We surmised that Lys-Cu was suitable to detect Cu<sup>2+</sup> in lysosomes. At the same time, we hypothesized that even the probe into the other neutral or alkaline organelle, the probe Lys-Cu will not imaging (in the red channel) of copper ion in this organelle.

### Response rate and selectivity

Notably, the reaction of the probe Lys-Cu with Cu<sup>2+</sup> was very rapid. As shown in Fig. 6, a marked increase in the fluorescence intensity was observed within seconds, and a maximal fluorescence

signal was obtained in two minute, indicating that the probe may be used to monitor  $\text{Cu}^{2+}$  in real time. This is the unique feature of probe **Lys-Cu** when compared to other known fluorescent  $\text{Cu}^{2+}$  ion probes<sup>10k</sup>.

The probe was treated with various metal ions to investigate the selectivity. Representative metal ions such as  $\text{K}^+$ ,  $\text{Mg}^{2+}$ ,  $\text{Na}^+$ ,  $\text{Ni}^{2+}$ ,  $\text{Pd}^{2+}$ ,  $\text{Zn}^{2+}$ ,  $\text{Ag}^+$ ,  $\text{Ca}^{2+}$ ,  $\text{Cu}^+$ ,  $\text{Fe}^{2+}$ ,  $\text{Co}^{2+}$ ,  $\text{H}_2\text{O}_2$ ,  $\text{NO}$  only induce minimum perturbation in fluorescence spectra of probe **Lys-Cu**. However, the addition of  $\text{Cu}^{2+}$  to probe **Lys-Cu** causes the largest fluorescence enhancement, both around 440 (Fig. S5A) and 580 nm (Fig. 7A). Thus, emissions from two channels are metal-ion dependent. This contributes considerably to the high selectivity of the probe, supporting the benefit of dual-channel fluorescence-enhanced emissions. Furthermore, the visible color changes of probe **Lys-Cu** is also metal-ion dependent (Fig. S6); thus, the probe could be employed for convenient visual sensing of  $\text{Cu}^{2+}$ . To further explore the effective applications of the probe, the fluorescence response of **Lys-Cu** to  $\text{Cu}^{2+}$  in the presence of typical competing ions was studied. As shown in Fig. 7B and Fig. S5B, when  $\text{Cu}^{2+}$  (30 equiv) was added to probe **Lys-Cu** in the presence of a wide variety of competing metal ions (30 equiv) most exhibited minimum interference in the detection of  $\text{Cu}^{2+}$ . Thereby, probe **Lys-Cu** is useful for selectively sensing  $\text{Cu}^{2+}$  even under competition from other related metal ions.

#### Fluorescence imaging of $\text{Cu}^{2+}$ in the living cells with **Lys-Cu**

Encouraged by the above prominent results of the spectroscopic data establishing that the probe can selectively respond to  $\text{Cu}^{2+}$  in aqueous solution, we evaluated **Lys-Cu** imaging assays in live cells, and fluorescence imaging experiments were carried out in living cells (SiHa cells) on confocal laser scanning microscopy.

The standard MTT assays for the probe **Lys-Cu** at different concentrations were conducted, and the results show that the probe exhibited low cytotoxicity after a long period (24 h) (Fig. S7). Thus, the favorable properties of the probe include high selectivity and low cytotoxicity, which may render the probe **Lys-Cu** suitable for imaging  $\text{Cu}^{2+}$  in living cells. We examine whether **Lys-Cu** functions in living cells. The utility of probe **Lys-Cu** for fluorescence imaging of  $\text{Cu}^{2+}$  in living cells was investigated (Fig. 8). Staining of SiHa cells with only probe **Lys-Cu** (5.0  $\mu\text{M}$ ) provided no significant fluorescence (Fig. 8a). By contrast, in Fig. 8b-e, the cells were pre-treated with  $\text{Cu}^{2+}$  in the growth medium for 30 min. The cells were then washed with PBS (pH=7.4) to remove the remaining  $\text{Cu}^{2+}$  and further incubated with probe **Lys-Cu** for 30 min. The resulting bright fluorescence image at blue channel and red channel demonstrates that probe **Lys-Cu** with suitable amphipathicity is cell membrane permeable and able to display a fluorescence turn-on response to  $\text{Cu}^{2+}$  in the living cells.

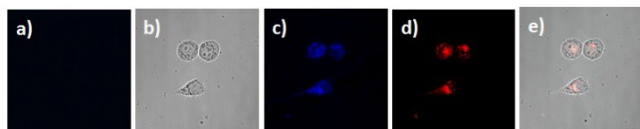


**Fig. 8** Brightfield and fluorescence images of SiHa cells stained with the probe **Lys-Cu**. a) only probe **Lys-Cu** fluorescence image from the red channel; b) brightfield image; c) fluorescence image from the blue channel in presence of  $\text{Cu}^{2+}$ ; d) fluorescence image from the red channel in presence of  $\text{Cu}^{2+}$ ; e) overlay of fluorescence blue channel, red channel and bright-field images.

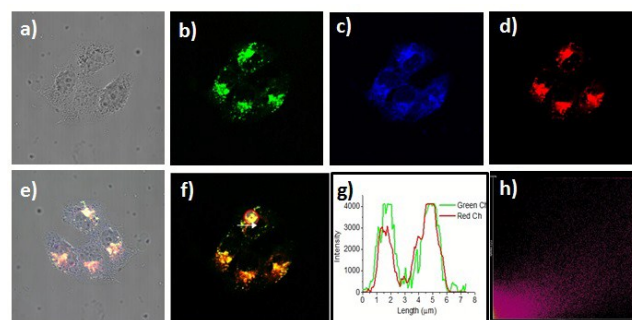


**Fig. 9** Brightfield and fluorescence images of SiHa cells stained with the probe **Lys-Cu** a) brightfield image; b) from green channel (lysosomes staining); c) from the blue channel; d) from the red channel; e) overlay of brightfield, green, blue and red channels; f) overlay of green and red channels; g) Intensity profile of linear region of interest across the SiHa cell costained with LysoTracker Green and red channel of **Lys-Cu**; h) Intensity scatter plot of green and red channels.

#### The ability to accumulate into lysosomes

Encouraged by the above promising results of two channel imaging, we decided to further examine the feasibility of the probe **Lys-Cu** to detect of  $\text{Cu}^{2+}$  in lysosomes. Colocalization experiments were performed by costaining SiHa cells with the commercial lysosome tracker LysoTracker Green and **Lys-Cu** in the presence of  $\text{Cu}^{2+}$  (Fig. 9). Green channel is the imaging of lysosomes by the tracker of LysoTracker Green (Fig. 9b). Bright fluorescence image at blue channel and red channel belong to the probe **Lys-Cu** imaging of  $\text{Cu}^{2+}$  (Fig. 9c and 9d). The merged image (Figure 9f) indicates that the staining of **Lys-Cu** fits well with that of lysosome tracker. The intensity profile of linear regions of interest across a SiHa cell in the two channels also varies in close synchrony (Fig. 9g). Moreover, the intensity scatter plot of green channel and red channel is high correlation with a high overlap Pearson's coefficient of 0.90 and Mander's overlap coefficient of 0.97 in the ROI (Fig.9h). The results suggest that probe **Lys-Cu** can readily permeate the cell membrane and can be located in lysosomes specifically. However, blue channel and green channel merged images (Fig. S8a) indicates that the staining of **Lys-Cu** blue channel did not overlap well with the image of lysosome tracker green channel. The intensity profile of linear regions of interest across a SiHa cell in the two channels was also not well (Fig. S8b) and the overlap Pearson's coefficient was only 0.71 and Mander's overlap coefficient of 0.90 in the ROI (Fig. S8c). The main reason is that due to the using of short-wavelength laser excitation, lead to the enhanced background noise of the cells, which results in a slightly decreasing colocalization coefficient of the blue channel in lysosomes.

## Experimental Section

### Materials and instruments

Compounds **4** and **5** were prepared according to a literature procedure.<sup>13a,14</sup> Unless otherwise stated, all reagents were purchased from commercial suppliers and used without further purification. Solvents used were purified by standard methods prior to use. Twice-distilled water was used throughout all experiments. High resolution mass spectrometric (HRMS) analyses were measured on a Finnigan MAT 95 XP spectrometer; NMR spectra were recorded on an AVANCE III 400 MHz Digital NMR Spectrometer, using TMS as an internal standard; Absorption spectra were obtained on a Shimadzu UV-2700 Power spectrometer; Photoluminescent spectra were recorded with a HITACHI F4600

fluorescence spectrophotometer with a 1 cm standard quartz cell; The fluorescence imaging of cells was performed with Nikon A1MP confocal microscopy; The pH measurements were carried out on a Mettler-Toledo Delta 320 pH meter; TLC analysis was performed on silica gel plates and column chromatography was conducted over silica gel (mesh 200-300), both of which were obtained from the Qingdao Ocean Chemicals.

#### Preparation of the stock and test solution

Unless otherwise noted, all the measurements were made according to the following procedure. A stock solution (1.0 mM) of **Lys-Cu** was prepared by dissolving the requisite amount of it in acetonitrile. In a 10 mL tube the test solution of compounds **Lys-Cu** was prepared by placing 0.1 mL of stock solution, 4.9 mL of acetonitrile, 3 mL of 0.1 M PBS buffer (different pH) and an appropriate volume of  $\text{Cu}^{2+}$  sample solution. After adjusting the final volume to 10 mL with distilled-deionized water, standing at room temperature 3 min, 3 mL portion of it was transferred to a 1 cm quartz cell to measure absorbance or fluorescence. The stock solutions of metal ions for selectivity experiments were prepared respectively by dissolving NaCl, KCl,  $\text{CaCl}_2$ ,  $\text{ZnCl}_2$ ,  $\text{CaCl}_2$ ,  $\text{AgNO}_3$ ,  $\text{MgCl}_2 \cdot 6\text{H}_2\text{O}$ ,  $\text{FeCl}_2 \cdot 4\text{H}_2\text{O}$ ,  $\text{CuSO}_4 \cdot 5\text{H}_2\text{O}$ ,  $\text{NiCl}_2 \cdot 6\text{H}_2\text{O}$ , and  $\text{CoCl}_2$  in twice-distilled water. The slight pH variations of the solutions were achieved by adding the minimum volumes of NaOH (0.1 M) or HCl (0.2 M).

#### Cytotoxicity assay

*In vitro* cytotoxicity was measured using the colorimetric methyl thiazolyl tetrazolium (MTT) assay on NIH3T3 cells. Cells were seeded into the 24-well tissue culture plate in the presence of 500  $\mu\text{L}$  Dulbecco's modified eagle medium (DMEM) supplemented with 10% fetal bovine serum (FBS) and 1% penicillin/streptomycin at 37 °C and 5%  $\text{CO}_2$  atmosphere for overnight and then incubated for 24 h in the presence of **Lys-Cu** at different concentrations (1, 5 and 10  $\mu\text{M}$ ). Then cells were washed with PBS buffer and 500  $\mu\text{L}$  supplemented DMEM medium was added. Subsequently, 50  $\mu\text{L}$  MTT (5 mg/mL) was added to each well and incubated for 4 h. Violet formazan was dissolved in 500  $\mu\text{L}$  sodium dodecyl sulfate solution in the water-DMF mixture. Absorbance of the solution was measured at 558 nm using a microplate reader. The cell viability was determined by assuming 100% cell viability for cells without **Lys-Cu**.

#### SiHa cells culture and imaging of $\text{Cu}^{2+}$ using probe **Lys-Cu**

SiHa cells were grown in MEM (modified Eagle's medium) supplemented with 10 % FBS (fetal bovine serum) in an atmosphere of 5%  $\text{CO}_2$  and 95% air at 37 °C. The cells were plated on 6-well plates and allowed to adhere for 24 h. immediately before the experiments; the cells were washed with phosphate-buffered saline (pH=7.4) buffer. Subsequently, the cells were incubated with 50  $\mu\text{M}$   $\text{CuSO}_4$  for 30 min at 37 °C, and then washed with PBS three times. After incubating with chemodosimeter **Lys-Cu** (5  $\mu\text{M}$ ) (containing 0.1 % DMSO as a cosolvent) for another 30 min at 37 °C, the HeLa cells were rinsed with PBS three times, and the fluorescence images were acquired through a Nikon A1MP confocal microscopy inverted fluorescence microscopy equipped with a cooled CCD camera.

#### Synthesis of compound 2

With an inert atmosphere of nitrogen, to a mixture of compound **1** (500 mg, 1.29 mmol, 1.0 equiv) in 1,4-dioxane (20 mL) was added  $\text{Pd}(\text{dppf})\text{Cl}_2$  (94.4 mg, 0.013 mmol, 0.1 equiv), potassium acetate (378 mg, 3.86 mmol, 3.0 equiv), bis(pinacolato)diboron (688 mg, 1.93 mmol, 1.5 equiv). The reaction was stirred for 10 h at 120 °C in an oil bath.  $\text{H}_2\text{O}$  (50 mL) was added and the mixture was extracted with 50 mL EtOAc thrice. The combined extracts were washed with water, brine and dried over  $\text{Na}_2\text{SO}_4$ . Concentration and chromatograph on silica gel (1:1 petroleum ether/ethyl acetate). This resulted in 401 mg (72 %) of compound **2** as a white solid.  $^1\text{H-NMR}$  (400 MHz,  $\text{CDCl}_3$ )  $\delta$  9.15 (dd,  $J = 8.5, 1.0$  Hz, 1H), 8.62 (dd,  $J = 7.3, 2.6$  Hz, 1H), 8.59 (d,  $J = 7.3$  Hz, 1H), 8.33 (d,  $J = 7.3$  Hz, 1H), 7.81 (dd,  $J = 8.4, 7.4$  Hz, 1H), 4.38 (s, 2H), 3.71 (s, 4H), 2.69 (m, 6H), 1.47 (s, 12H).  $^{13}\text{C NMR}$  (101 MHz,  $\text{CDCl}_3$ )  $\delta$  164.4, 135.8, 135.3, 135.1, 134.0, 130.9, 129.8, 127.9, 127.1, 124.6, 122.5, 84.6, 83.0, 66.9, 56.1, 53.7, 25.0, 24.6. HRMS (ESI)  $m/z$  calcd for  $\text{C}_{24}\text{H}_{30}\text{BN}_2\text{O}_5$   $[\text{M}+\text{H}]^+$ : 437.2252; found 437.2244.

#### Synthesis of compound **Lys-Cu**

With an inert atmosphere of nitrogen, to a mixture of compound **3** (103 mg, 0.19 mmol, 1.0 equiv) in toluene (5 mL) was added  $\text{Pd}(\text{PPh}_3)_4$  (22 mg, 0.019 mmol, 0.1 equiv), Potassium acetate (1 mL, 2 mol/L) and compound **2** (100 mg, 0.23 mmol, 1.2 equiv). The reaction was stirred for 10 h at 120 °C in an oil bath. 50 mL  $\text{H}_2\text{O}$  was added and the mixture was extracted with 50 mL ethyl acetate thrice. The combined extracts were washed with water, brine and dried over  $\text{Na}_2\text{SO}_4$ . Concentration and chromatograph on silica gel (1:40  $\text{CH}_2\text{Cl}_2/\text{MeOH}$ ). This resulted in 101 mg (70 %) of **Lys-Cu** as a green solid.  $^1\text{H-NMR}$  (400MHz,  $\text{DMSO}-d_6$ )  $\delta$  8.65 -8.51 (m, 2H), 8.32 (d,  $J = 8.2$  Hz, 1H), 7.93-7.91 (m, 3H), 7.75 - 7.65 (m, 1H), 7.22 (d,  $J = 7.8$  Hz, 1H), 6.51 (d,  $J = 8.8$  Hz, 2H), 6.41 (d,  $J = 8.0$  Hz, 3H), 4.42 (s, 2H), 4.23 (t,  $J = 6.8$  Hz, 2H), 3.54 (s, 4H), 3.35 (s, 4H), 2.60 (t,  $J = 6.9$  Hz, 2H), 2.49 - 2.39 (m, 3H), 1.11 (t,  $J = 6.9$  Hz, 12H);  $^{13}\text{C NMR}$  (101 MHz,  $\text{CDCl}_3$ )  $\delta$  165.6, 164.3, 164.0, 153.9, 151.8, 149.1, 145.7, 138.8, 134.2, 132.4, 131.3, 130.8, 130.5, 129.9, 128.8, 128.2, 127.9, 127.1, 124.3, 124.2, 123.0, 122.1, 108.1, 104.0, 98.2, 67.1, 66.1, 56.2, 53.9, 44.4, 37.3, 29.7; HRMS (ESI)  $m/z$  calcd for  $\text{C}_{46}\text{H}_{48}\text{N}_6\text{O}_5$   $[\text{M}+\text{H}]^+$ : 765.3764; found 765.3809.

#### Conclusions

The probe **Lys-Cu** was developed as a fluorescence-enhanced and lysosome-targeted  $\text{Cu}^{2+}$  probe with unique dual-channel emissions. The addition of  $\text{Cu}^{2+}$  to **Lys-Cu** results in not only a large fluorescence enhancement at 440 nm because of inhibition of a quenching PET channel, but also a dramatic fluorescence enhancement around 580 nm as a result of the trigger of rhodamine B ring-opened form formation. The metal-ion-dependent dual-channel fluorescence-enhanced response contributes substantially to the high selectivity of **Lys-Cu**. Notably, the probe was located specifically in lysosomes while dual-channel imaging  $\text{Cu}^{2+}$  in lysosomes. Therefore, the probe is feasible for fluorescently monitoring  $\text{Cu}^{2+}$  level changes in lysosomes and probably for studying diseases associated with disorders of  $\text{Cu}^{2+}$  metabolism in lysosomes. In addition, this work establishes a robust strategy for dual-emission fluorescent probes, and the modularity of the strategy may allow it to be extended for other types of metal ion by judicious selection of the suitable reaction sites. Work along these lines is under progress. We believe that the dual-channel signaling mechanism of probe **Lys-Cu** should lead to the development of powerful probes for other metal ions with

fluorescence-enhanced dual-channel emissions for exciting applications in diverse fields.

14 L. Wang, M. Sibrian-Vazquez, J. O. Escobedo, J. Wang, R. G. Moore and R. M. Strongin *Chem. Comm.*, 2015, **51**, 1697-1700.

## Acknowledgements

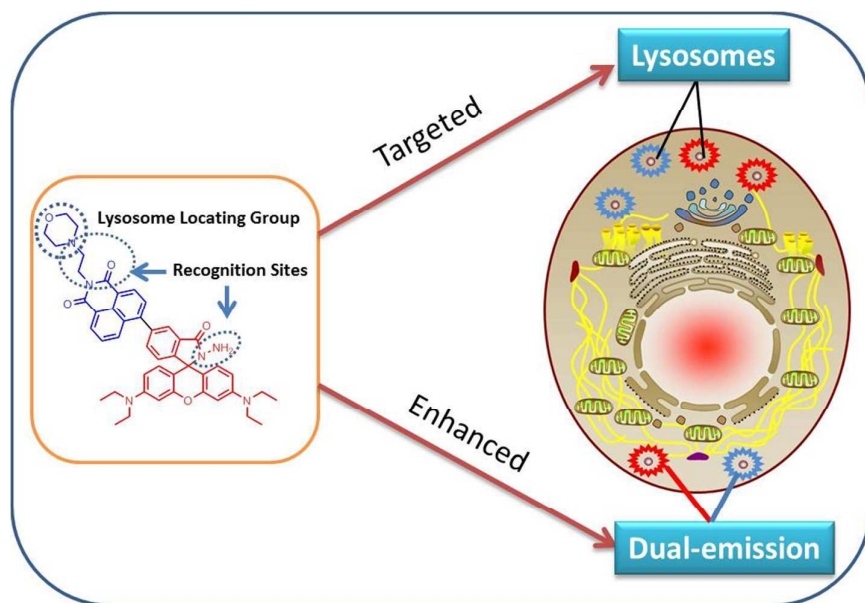
This work was financially supported by NSFC (21172063, 21472067), The Natural Science Foundation of Shandong Province, China (100021715), and the startup fund of University of Jinan.

## Notes and references

- 1 R. S. Britton Semin, *Liver. Dis.*, 1996, **16**, 3-12.
- 2 S. Lutsenko, A. Gupta, J. L. Burkhead and V. Zuzel, *Arch. Biochem. Biophys.*, 2008, **476**, 22-32.
- 3 S. Sisodiya, *Nat. Rev. Neurol.*, 2011, **7**, 129-130.
- 4 K. J. Barnham, C. L. Masters and A. I. Bush, *Nat. Rev. Drug. Discov.*, 2004, **3**, 205-214.
- 5 P. V. E. Van den Berghe, D. E. Folmer, H. E. M. Malingre, E. Van Beurden, A. E. M. Klomp, B. V. De Sluis, M. Merckx, R. Berger and L. W. J. Klomp, *Biochem. J.*, 2007, **407**, 49-59.
- 6 L. Arce, A. Domínguez-Vidal, V. Rodríguez-Estévez, S. López-Vidal, M. J. Ayora-Cañada and M. Valcárcel, *Anal. Chim. Acta*, 2009, **636**, 183-189.
- 7 Y. Liu, P. Liang and L. Guo, *Talanta*, 2005, **68**, 25-30.
- 8 A. A. Ensafi, T. Khayamian, A. Benvidi and E. Mirmomtaz, *Anal. Chim. Acta*, 2006, **561**, 225-232.
- 9 W. L. Cheng, J. W. Sue, W. C. Chen, J. L. Chang and J. M. Zen, *Anal. Chem.*, 2010, **82**, 1157-1161.
- 10 (a) D. T. Quang and J. S. Kim, *Chem. Rev.*, 2010, **110**, 6280-6301; (b) W. Shi and H. Ma, *Chem. Comm.*, 2012, **48**, 8732-8744. (c) C. Yu, J. Zhang, R. Wang and L. Chen, *Org. Biomol. Chem.*, 2010, **8**, 5277-5279; (d) Y. Liu, Y. Sun, J. Du, X. Lv, Y. Zhao, M. Chen, P. Wang and W. Guo, *Org. Biomol. Chem.*, 2011, **9**, 432-437; (e) W. Y. Liu, H. Y. Li, B. X. Zhao and J. Y. Miao, *Org. Biomol. Chem.*, 2011, **9**, 4802-4805; (f) L. Zhang, Y. Zhang, M. Wei, Y. Yi, H. Li and S. Yao, *New J. Chem.*, 2013, **37**, 1252-1257; (g) M. Taki, S. Iyoshi, A. Ojida, I. Hamachi and Y. Yamamoto, *J. Am. Chem. Soc.*, 2010, **132**, 5938-5939; (h) S. C. Dodani, S. C. Leary, P. A. Cobine, D. R. Winge and C. J. Chang, *J. Am. Chem. Soc.*, 2011, **133**, 8606-8616; (i) L. Huang, X. Wang, G. Xie, P. Xi, Z. Li, M. Xu, Y. Wu, D. Bai and Z. Zeng, *Dalton Trans.*, 2010, **39**, 7894-7896; (j) M. Yu, M. Shi, Z. Chen, F. Li, X. Li, Y. Gao, J. Xu, H. Yang, Z. Zhou, T. Yi and C. Huang, *Chem.-Eur. J.*, 2008, **14**, 6892-6900; (k) Y.-B. Ruan, C. Li, J. Tang and J. Xie, *Chem. Commun.*, 2010, **46**, 9220-9222; (l) Q. Qu, A. Zhu, X. Shao, G. Shi and Y. Tian, *Chem. Commun.*, 2012, **48**, 5473-5475; (m) W. Lin, L. Long, B. Chen, W. Tan and W. Gao *Chem. Commun.*, 2010, **46**, 1311-1313; (n) W. Y. Liu, H. Y. Li, B. X. Zhao and J. Y. Miao, *Analyst*, 2012, **137**, 3466-3469; (o) Y. Li, X. Zhang, B. Zhu, J. Xue, Z. Zhu and W. Tan, *Analyst*, 2011, **136**, 1124-1128; (p) X. Wang, X. Ma, Z. Yang, Z. Zhang, J. Wen, Z. Geng and Z. Wang, *Chem. Commun.*, 2013, **49**, 11263-11265; (q) P. Li, H. Zhou and B. Tang, *J. Photochem. Photobiol. A: Chem.*, 2012, **249**, 36-40; (r) Y. Li, Y. Zhao, W. Chan, Y. Wang, Q. You, C. Liu, J. Zheng, J. Li, S. Yang and R. Yang, *Anal. Chem.*, 2015, **87**, 584-591; (s) Z. Xu, J. Yoon and D. R. Spring, *Chem. Commun.*, 2010, **46**, 2563-2565; (t) X. Guan, W. Lin and W. Huang, *Org. Biomol. Chem.*, 2014, **12**, 3944-3949
- 11 (a) G. Li, D. Zhu, L. Xue and H. Jiang *Org. Lett.*, 2013, **15**, 5020-5023; (b) R. Sun, W. Liu, Y. J. Xu, J. M. Lu, J. F. Ge and M. Ihara, *Chem. Comm.*, 2013, **49**, 10709-10711; (c) H. Yu, Y. Xiao and L. Jin, *J. Am. Chem. Soc.*, 2012, **134**, 17486-17489; (d) H. Zhu, J. Fan, Q. Xu, H. Li, J. Wang, P. Gao and X. Peng, *Chem. Comm.*, 2012, **48**, 11766-11768; (e) D. Song, J. M. Lim, S. Cho, S. J. Park, J. Cho, D. Kang, S. G. Rhee, Y. You and W. Nam, *Chem. Comm.*, 2012, **48**, 5449-5451; (f) H. Zhu, J. Fan, S. Zhang, J. Cao, K. Song, D. Ge, H. Dong, J. Wang and X. Peng, *Biomater. Sci.*, 2014, **2**, 89-97
- 12 (a) B. Zhu, C. Gao, Y. Zhao, C. Liu, Y. Li, Q. Wei, Z. Ma, B. Du and X. Zhang, *Chem. Comm.*, 2011, **47**, 8656-8658; (b) X. L. Liu, X. J. Du, C. G. Dai and Q. H. Song, *J. Org. Chem.*, 2014, **79**, 9481-9489
- 13 (a) J. Woo, G. Kim, K. Quintero, M. P. Hanrahan, H. Palencia and H. Cao, *Org. Biomol. Chem.*, 2014, **12**, 8275-8279; (b) H. Yu, Y. Xiao and H. Guo, *Org. Lett.*, 2012, **14**, 2014-2017.

## A Dual-Emission Fluorescence-Enhanced Probe for Imaging Copper(II) Ions in Lysosomes

Mingguang Ren, Beibei Deng, Jian-Yong Wang, Zhan-Rong Liu, Weiying Lin\*



We have developed the first example of a fluorescence-enhanced and Lysosomal-targeted  $\text{Cu}^{2+}$  probe (**Lys-Cu**) with unique dual-channel emissions. Fluorescence imaging shows that **Lys-Cu** is membrane-permeable and suitable for visualization of  $\text{Cu}^{2+}$  in lysosomes of living cells with dual-channel imaging.